Diffusion effects of alumina on microstructures and positive temperature coefficient resistivity (PTCR) characteristics of barium–strontium titanate ceramics

P. BOMLAI, N. SIRIKULRAT*
Department of Physics, Faculty of Science, Chiang Mai University, Chiang Mai 50200, Thailand
E-mail: scphi003@chiangmai.ac.th

It is well known that donor-doped barium titanate ceramics show positive temperature coefficient resistivity (PTCR) characteristics, resulting in a sudden change of resistivity near the Curie temperature (T_C) [1–6]. Moreover, the T_C can be shifted to lower temperatures by adding $SrTiO_3$ or to higher temperatures by adding $PbTiO_3$ [7]. The PTCR effects can be improved significantly by the presence of the acceptor dopants at the grain boundary [8]. In particular, the resistance jumping can be enhanced considerably when ceramics are doped with 3d elements, such as Mn, Fe and Cu, acting as acceptors resulting from an increase in the surface state acceptor density [9]. Daniels and Wernicke reported the influence of 3d transition elements on the formation of an insulating grain boundary layer, rich in Ba-vacancies, arising as a consequence of incorporation of the 3d elements into the lattice [3]. Recently, a new process, the so-called vapor-doping method, involving doping with a vapour dopant has been used and a great improvement in the PTCR effects found [8, 10–12]. Doping processes are very important and depend on the electrical properties and microstructures of materials [13]. Many researchers have used Al_2O_3 as a sintering aid together with excess TiO_2 and SiO_2 to create a liquid phase and reduce the sintering temperature [14–17]. However, most investigations [14–20] prepared PTCR specimens by the addition of alumina mixed together with other raw materials ($BaCO_3$, TiO_2, etc.). Cheng *et al*. [16] added 12.5 mol% AST (Al_2O_3–SiO_2–TiO_2) and obtained high PTCR characteristics, low resistivity at room temperature and a small grain size of about 10 μm. However, we repeated their experiment and found a low PTCR response and a high resistivity at room temperature. Owing to the tremendous development in the applications of PTCR materials, PTCR characteristics have been a very important research topic. From the vapor-doping method, it is supposed that some alumina might diffuse into the specimens during sintering to give rise to the observed effects on the PTCR properties. The objective of this study, therefore, is to investigate the effects of alumina diffusion on the microstructures and PTCR characteristics of barium–strontium titanate (BST) ceramics when samples were prepared by sintering with an alumina surrounding. A number of effects due to the alumina on the PTCR characteristics were found.

Samples were prepared by using the conventional mixing oxide process. The starting materials of $BaCO_3$, $SrCO_3$, TiO_2, Sb_2O_3 and SiO_2 (Aldrich Chemical Company Inc., >99.9% purity) in a molar composition of $0.8BaCO_3 + 0.2SrCO_3 + 1.01TiO_2 + 0.0015Sb_2O_3 + 0.03SiO_2$ were ball-milled with zirconia grinding media and ethanol in a polypropylene jar for 24 h. The mixture was dried, crushed and then calcined in air at 1100 °C for 2 h. The calcined powder was blended with 3 wt.% polyvinyl alcohol (PVA) and then pressed into pellets 15 mm in diameter. Two types of surrounding powders were used for the sintering process. Some pellets were placed on Sb-doped BST powder in crucible A (samples A), while some were placed on alumina powder in crucible B (samples B). All of the samples were sintered in air in the same furnace at 1400 °C (at lower temperatures, almost no effect was found) at increasing times of 2, 4, and 8 h. Scanning electron microscopy (SEM; JEOL JSM-840A) was used to determine the microstructure of the samples. The dc resistance change of the specimens as a function of temperature was measured using a digital multimeter (Agilent 34401A) and a suitable power supply; electrodes were applied using silver paste. The measurements were carried out at temperature ranging from room temperature to ~300 °C; a silicone oil bath was used to heat the samples and a digital thermometer (Fluke S50) with a K-type thermocouple was used to monitor temperature. The impedance of the materials as a function of frequency was measured by an impedance analyzer (HP model LF 4192A) at room temperature. The amount of alumina at the grain boundaries in the samples was determined using backscattered electron images (BEI) and energy dispersive X-ray analysis (EDX; Camscan Series 4, with Oxford Instruments UTW EDX detector/ISIS Software Series 300 for microanalysis and digital image capture).

The results from the experiments show that both the microstructures and electrical properties of samples A and B are significantly different. The variation of grain size with both sintering time and the surrounding powder are shown in Fig. 1, as determined from SEM micrographs using a linear intercept method, Table I. The grains of samples A are consistently fine, smaller than those of samples B. As the sintering time increases, the grain size of samples A approaches a constant value of 7–9 μm, whereas the grain size of samples B continues

*Author to whom all correspondence should be addressed.

0022–2461

TABLE I Calculated parameters of the samples with various sintering times and surrounding powders

Samples	Mean grain size (μm)	R_g (Ω)	R_{gb} (Ω)	ρ_{RT} (Ω cm)	ρ_{max} (Ω cm)	$\log(\rho_{max}/\rho_{RT})$ (orders)
A–2 h	7.1	3.3	2.9	39	1.0×10^5	3.4
A–4 h	8.5	3.6	3.6	54	7.3×10^6	5.1
A–8 h	8.9	3.8	5.4	66	6.2×10^6	5.0
B–2 h	12.4	2.2	5.5	57	4.5×10^5	3.9
B–4 h	18.2	2.1	42.6	309	1.8×10^8	5.8
B–8 h	40.5	2.4	54.2	391	2.0×10^7	4.7

The mean grain size is calculated from Fig. 1. The impedance data (R_g and R_{gb}) are calculated from Fig. 4. The ρ_{RT}, ρ_{max} and $\log(\rho_{max}/\rho_{RT})$ values are calculated from Fig. 5.

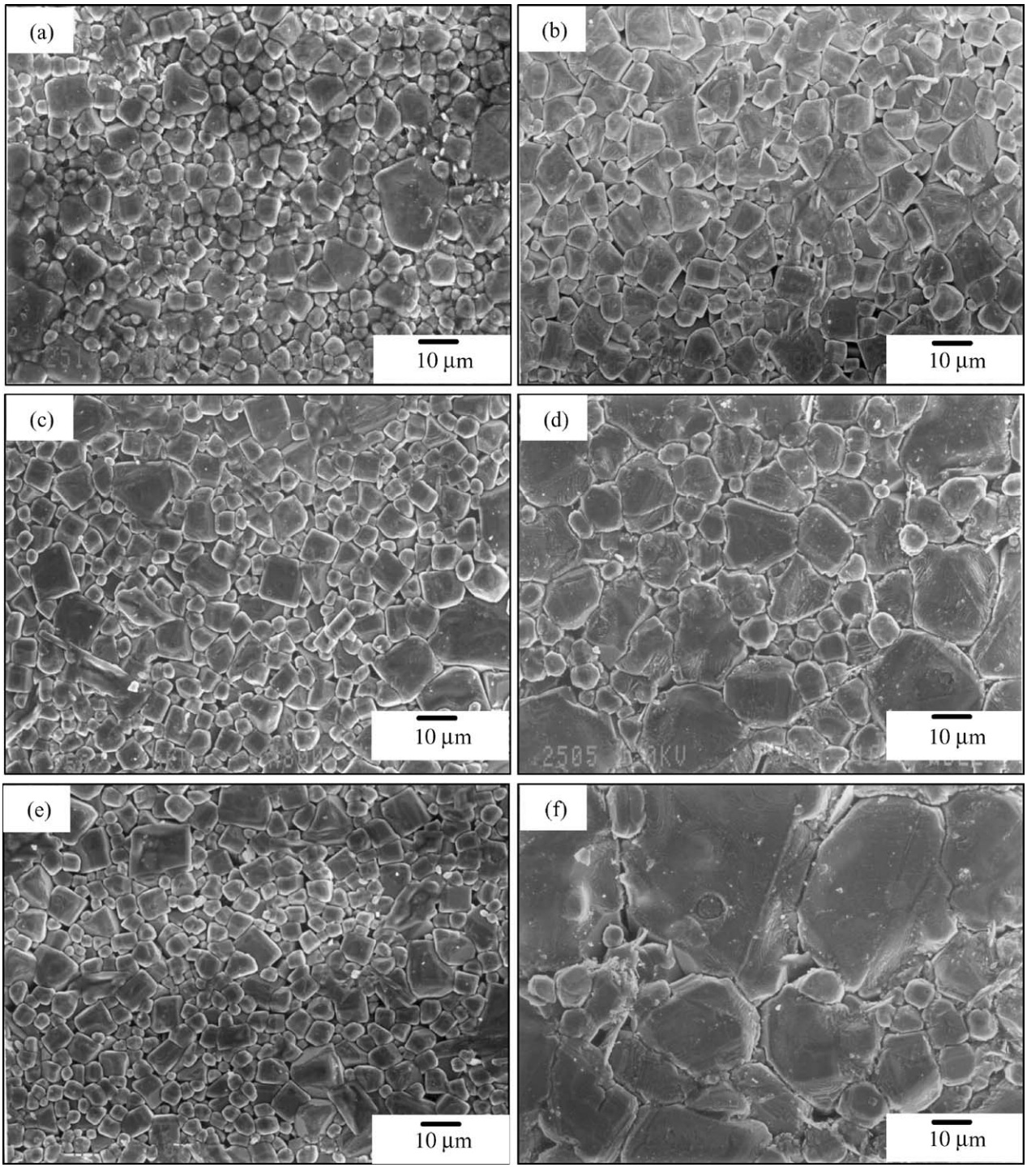

Figure 1 SEM micrographs of the grains of both BST samples at various sintering times: (a), (c) and (e) Samples A sintered for 2, 4 and 8 h. (b), (d) and (f) Samples B sintered for 2, 4 and 8 h.

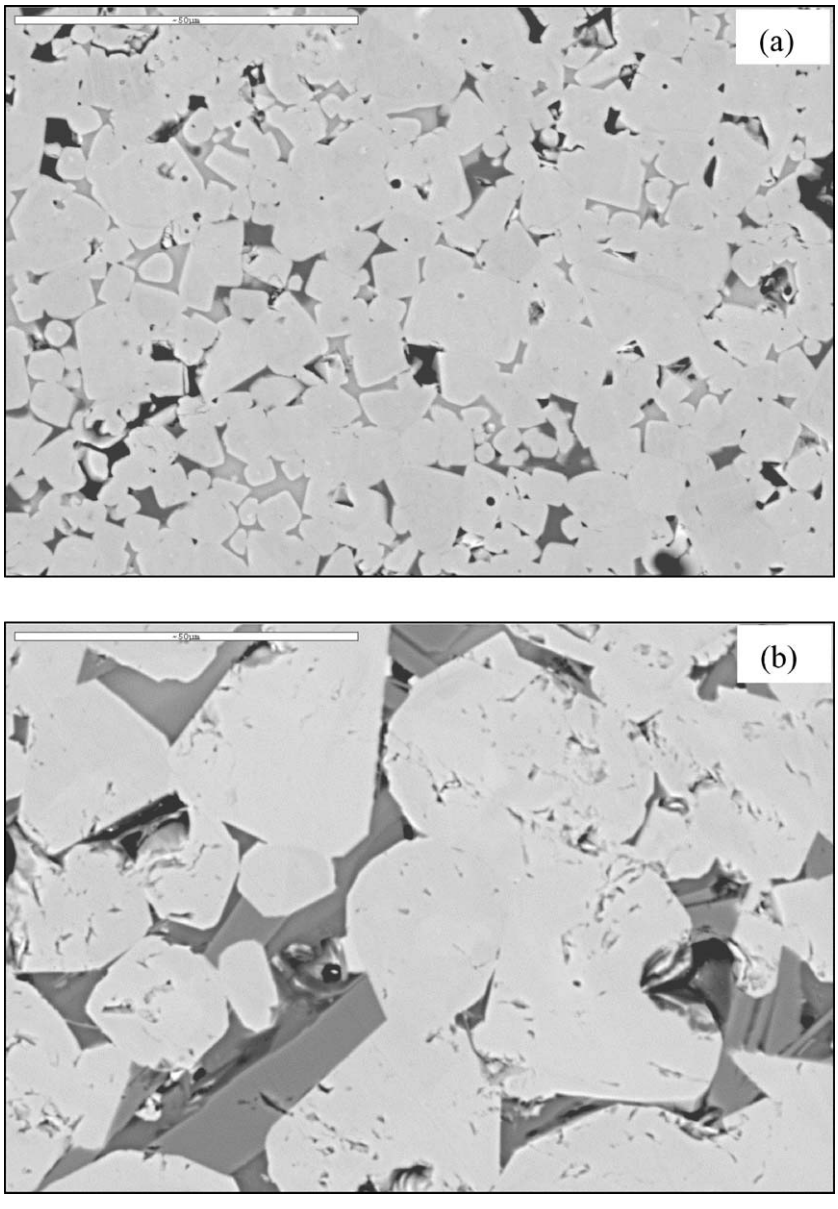

Figure 2 Back-scattered electron micrographs of the BST samples sintered with different surrounding powders at 1400 °C for 4 h: (a) Samples A (BST surrounding). (b) Samples B (alumina surrounding).

to increase. The grains of samples B show an anomalos growth with a grain size of up to 40 μm when sintered for 8 h. This fact suggests that mass transportation or diffusion of the surrounding alumina contributes to the increase in the average grain size of samples B.

The results from our BEI, EDX analyses and impedance measurements demonstrate alumina diffusing to the grain boundaries of the BST ceramics when the alumina sintering surrounding was used. The micrographs of BEI (Fig. 2) show a sharp difference in the grain features between samples A and B. While there are only small spaces and structure in the small-grain boundaries of the ceramics without the alumina sintering (samples A), the big-grain boundaries of the alumina-surrounding-sintered ceramics (samples B) are full of large spaces which are filled with second-phase structures. A detailed analysis using EDX (Fig. 3 and Table II) indicates that in samples B the intergranular structure, in a thickness of about 3–20 μm, is of Al-contained second phases such as an Al–Si-rich phase and an Al-Ba/Ti phase, as indicated in Fig. 3. In contrast, the second phase in samples A are $Ba_6Ti_{17}O_{40}$ and $Ba_2TiSi_2O_8$ [21]. The data in Table II show that Al is mainly located in the grain boundaries with only a few (%) in the grain interior. Furthermore, the concentration of Al in the grain boundaries is comparable with those of the main original ceramic elements such as Ba, Si and Ti. All of these results indicate that Al from the alumina surrounding diffuses into the ceramics during the sintering process, mainly along the grain boundaries, to form Al-rich-containing second phases.

TABLE II Quantitative results from EDX analysis of samples B sintered for 4 h (refer to Fig. 3)

	Normalized (at%)					
Sample composition	Ba	Ti	Sr	Al	Si	Sb
Grain interior	39.2	49.5	10.8	0.2	0.0	0.2
Grain boundary region (1)	22.1	12.6	–	37.7	27.5	–
Grain boundary region (2)	30.9	6.4	–	39.7	24.2	–
Grain boundary region (3)	25.1	65.7	0.5	8.6	0.03	0.04

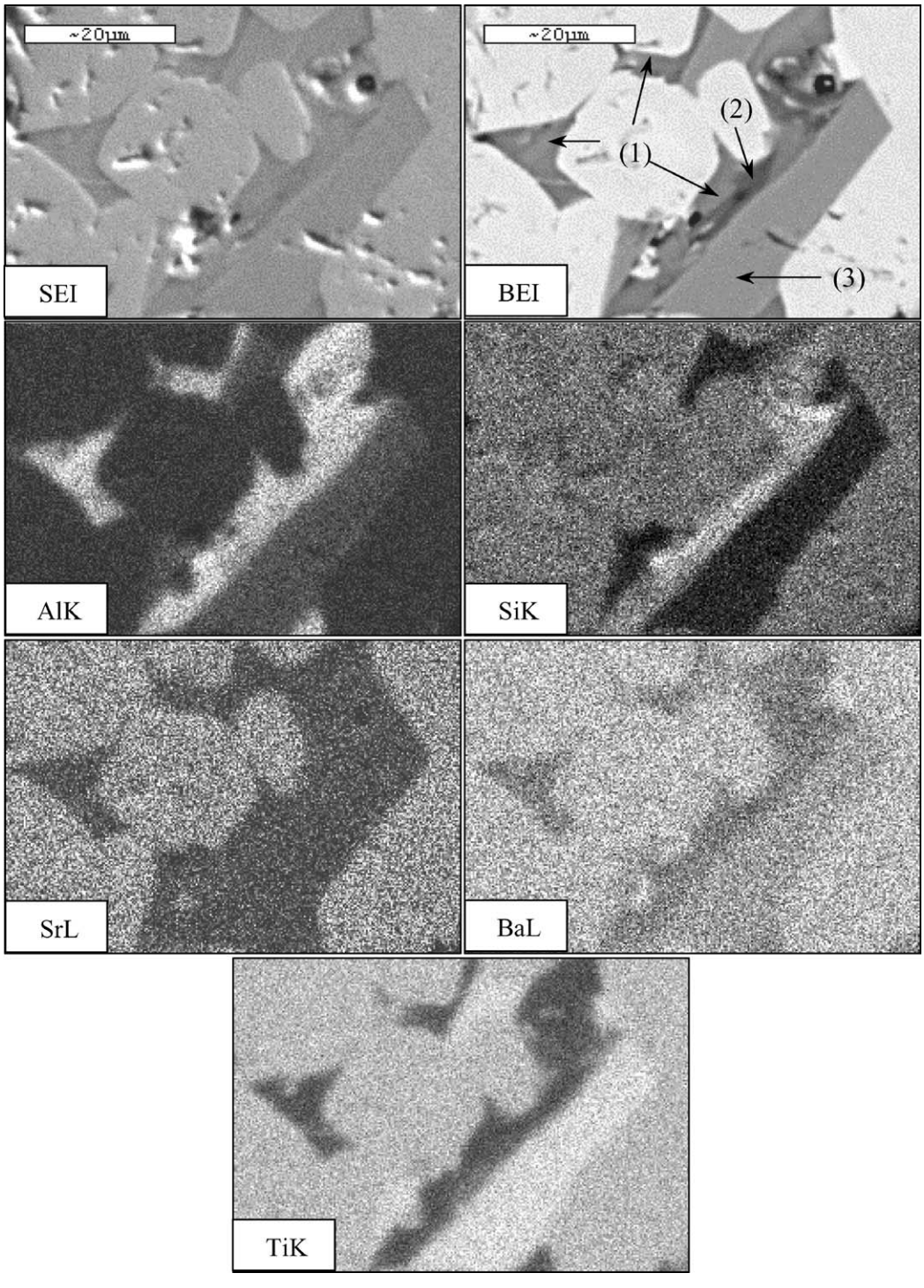

Figure 3 X-ray mapping of samples B sintered for 4 h ((1) and (2) are Al–Si-rich phases, (3) is Al-Ba/Ti phase, SEI is secondary electron image, BEI is back-scattered electron image, AlK is aluminium Kα, SiK is silicon Kα, SrL is strontium Lα, BaL is barium Lβ, TiK is titanium Kα).

Complex-plane impedance as a function of frequency was analyzed for the grain interior and boundary resistances. For *RC*-parallel systems wherein the ceramic–electrode interface resistance is negligible, the impedance (Z) is given by [22, 23]

$$Z = Z' - \mathrm{j}Z'' \tag{1}$$

then

$$Z = R_{\mathrm{g}} + \frac{1}{\left(\frac{1}{R_{\mathrm{gb}}}\right) + \mathrm{j}\omega C_{\mathrm{gb}}} \tag{2}$$

where Z' is the real part and Z'' the imaginary part of the total impedance, R_{g} the intra-grain resistance, R_{gb} the grain boundary resistance, and C_{gb} the grain boundary capacitance. The impedance diagrams of samples A and B at room temperature are shown in Fig. 4, and the relevant data calculated using formulae (1) and (2) are shown in Table I. The grain resistances of both samples are unchanged. However, the grain boundary resistance increases slightly for samples A and significantly for samples B with increasing sintering time. After 4 h of sintering, the grain boundary resistance of samples B is considerably greater than that of samples A. This indicates that insulating alumina diffuses to the grain

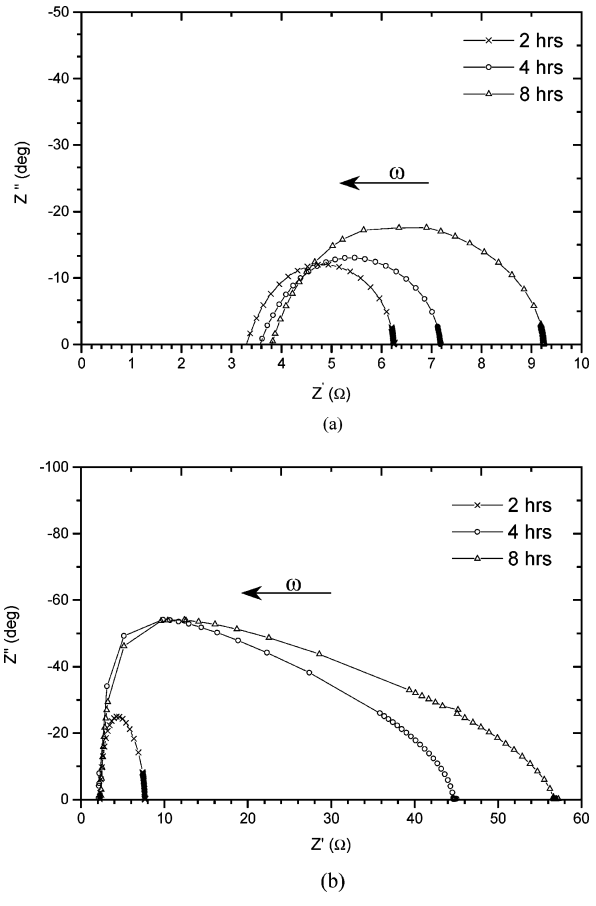

Figure 4 Impedance spectra of the BST samples at different sintering times, as recorded at room temperature (Z' means the real part of the total impedance, Z'' means the imaginary part of the total impedance). (a) Samples A. (b) Samples B.

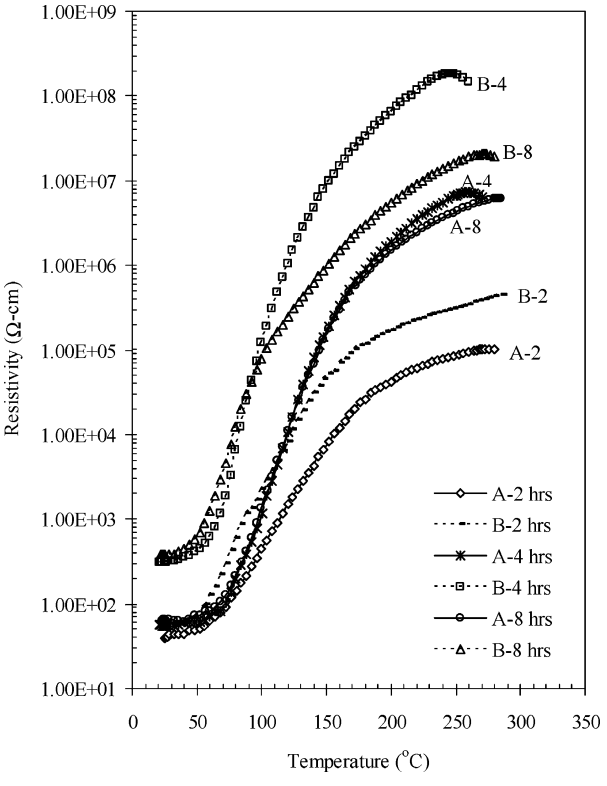

Figure 5 The resistivity–temperature characteristics of the samples sintered for various sintering times with the different surrounding powders (the short flat part of each curve over the temperature range below 40 °C is taken as the room-temperature resistivity, whereas the highest point of each curve is taken as the maximum resistivity).

boundaries to increase the resistance as the sintering time increases. Additionally, the diffused alumina can also decrease the grain interior resistance resulting from the aluminum-trapping impurities, such as Na, Cr, K, and Fe, which are harmful to the PTCR properties in the raw materials [19].

The effect of the alumina diffusion on the microstructure of the BST ceramics is seen not only in the grain growth but also in the grain shape. The grain shape became rounder (Fig. 1) when the ceramics were sintered in an alumina surrounding. It is considered that liquid-phase sintering occurred due to the low melting point of the second phases at the grain boundaries. The liquid phase would facilitate absorption of grain-growth inhibitors (e.g. the *n*-dopant and other impurities), thus favoring grain growth. While addition of aluminium into the ceramics has already been found to increase the grain size [20], we have found that sintering in an alumina surrounding has the same effect. Nonuniform grain growth was found in the 8-h-sintered samples B (Fig. 1f). This might be due to non-uniform wetting of the grain from the liquid when the grains grew too rapidly, giving rise to nonuniform absorbtion of the inhibitors [20].

The electrical resistivities of samples A and B as a function of temperature for various sintering times are shown in Fig. 5 and Table I. All samples exhibit PTCR behavior with the T_C of samples B slightly lower (50–60 °C) than that of samples A (65–70 °C). The room-temperature resistivity (ρ_{RT}), maximum resistivity (ρ_{max}), and the PTCR jump (the ratio of log (ρ_{max}/ρ_{RT})) depend on the sintering time and thus the diffusion of alumina. Both ρ_{RT} and ρ_{max} for all samples increase as the sintering time is increased up to 4 h. However, ρ_{max} decreases slightly for samples A and decreases markedly for samples B when the sintering time increases up to 8 h. This indicates that the diffusion of alumina relates to the increase in ρ_{RT}. A jump of the maximum resistivity is found to be about 5.8 orders of magnitude for the 4 h sintering samples B. It is obvious that the resistivity jump of the samples B was greater than that of the samples A. For these reasons, it can be concluded that alumina diffusion can positively improve the PTCR effect. The temperature of maximum resistivity (T_{max}) shifts slightly towards a lower temperature as the sintering time increases when the alumina sintering surrounding is used.

According to Heywang's model, the PTCR property of ceramic samples primarily arises from the presence of the Schottky barrier at the grain boundary [1, 16]. Kutty and Hari used alumina as an additive mixed with other raw materials (but without silicon) to make PTCR ceramics, and found that second phases were formed and defects acted as acceptors. However, their alumina addition [24] resulted in higher T_{max} and lower ρ_{max}. The enhancement of the PTCR response by alumina diffusion found in this investigation is also thought to be due to the diffused alumina acting as an electron trap, and increases with the surface state density. Thus, the increase in ρ_{RT} and ρ_{max} and the decrease in T_{max} with sintering time and diffusion of alumina can be

explained by the increase in the surface state density or the increase in the effective electron traps in the grain boundary region [20, 25, 26]. The decrease in ρ_{max}, particularly for samples B, after sintering for 8 h may be caused by the increase in grain size, leading to a decrease in the amount of grain boundaries per unit length [27].

It can be concluded that surrounding alumina in the sintering of the BST ceramics leads to the diffusion of alumina into the grain boundaries. Therefore, the diffused alumina can improve the PTCR effect in the ceramics during the sintering process. The effects of alumina diffusion can be summarized as follows: (i) the diffusion effect is shown only when the sintering temperature is as high as 1400 °C; (ii) the ρ_{RT}, ρ_{max}, and improvement of PTCR jumping increase with sintering time in the range of 2–4 h; however, the PTCR properties decrease if the sintering time is extended to 8 h; and (iii) the diffusion leads to an increase in grain size and formation of a liquid phase containing alumina, silicon and excess titanium. The enhancement of the PTCR properties due to the alumina diffusion is attributed to diffused-alumina-induced defects as well as an increase in the surface state density.

Acknowledgments

The authors would like to express their sincere thanks to the Thailand Research Fund, the National Metal and Materials Technology Centre (MTEC), the Graduate School, Chiang Mai University and the Ministry Staff Development Project of the Ministry of University Affairs, Thailand, for their financial support. We also wish to thank Dr L. D. Yu and Dr R. Molloy for their useful comments.

References

1. W. HEYANG, *J. Amer. Ceram. Soc.* **47** (1964) 484.
2. G. GOODMAN, *ibid.* **46** (1963) 48.
3. J. LILINGSWORTH, H. M. AL-ALLAK, A. W. BRINKMAN and J. WOODS, *J. Appl. Phys.* **67** (1990) 2088.
4. O. SABURI, *J. Amer. Ceram. Soc.* **44** (1961) 54.
5. *Idem.*, *J. Phys. Soc. Jpn.* **14** (1959) 1159.
6. M. DROFENIK and S. UREK, *J. Eur. Ceram. Soc.* **19** (1999) 913.
7. M. KUWABARA and M. KUMAMOTO, *J. Amer. Ceram. Soc.* **66** (1983) C214.
8. J. QI, W. CHEN, Y. WU and L. LI, *ibid.* **81** (1998) 437.
9. J. QI, Z. GUI, Q. ZHU, Y. WANG, Y. WU and L. LI, *Sens. Actuators A* **100** (2002) 244.
10. S. CHATTERJEE and H. S. MAITI, *Mater. Chem. Phys.* **67** (2001) 294.
11. J. QI, Z. GUI, Y. WU and L. LI, *Sens. Actuators A* **93** (2001) 84.
12. J. QI, Z. QING, Y. WANG, Y. WU and L. LI, *Solid State Commun.* **120** (2001) 505.
13. J. QI, Z. GUI, Y. WANG, Y. WU and L. LI, *Mater. Sci. Eng. B* **95** (2002) 283.
14. H. A. SAUER and J. R. FISHER, *J. Amer. Ceram. Soc.* **43** (1960) 297.
15. H. F. CHENG, *J. Appl. Phys.* **66** (1989) 1382.
16. H. F. CHENG, T. F. LIN, C. T. HU and I. N. LIN, *J. Amer. Ceram. Soc.* **76** (1993) 827.
17. J. K. LEE, J. S. PARK, K. S. HONG, K. H. KO and B. C. LEE, *ibid.* **85** (2002) 1173.
18. N. H. CHAN, R. K. SHARMA and D. M. SMYTH, *ibid.* **65** (1982) 167.
19. S. ATSUMI and S. WADA, US Patent No. 4 222 783 (1980).
20. H. M. AL-ALLAK, T. V. PARRY, G. J. RUSSELL and J. WOODS, *J. Mater. Sci.* **23** (1988) 1083.
21. P. BOMLAI, N. SIRIKULRAT and T. TUNKASIRI, *ibid.* **39** (2004) 1831.
22. B. HUYBRECHTS, K. ISHIZAKI and M. TAKATA, *ibid.* **30** (1995) 2643.
23. T. Y. TSENG and Y. Y. LU, *Ceram. Int.* **14** (1988) 195.
24. T. R. N. KUTTY and N. S. HARI, *Mater. Lett.* **34** (1998) 43.
25. G. H. JONKER, *Mater. Res. Bull.* **2** (1967) 437.
26. Y. Y. LU, C. H. LAI and T. Y. TSENG, *J. Amer. Ceram. Soc.* **77** (1994) 2461.
27. T. FUKAMI and H. TSUCHIYA, *Jpn. J. Appl. Phys.* **18** (1979) 735.

Received 19 December 2003
and accepted 22 July 2004